Materials Advances

ROYAL SOCIETY OF CHEMISTRY

PAPER

View Article Online
View Journal | View Issue

Cite this: *Mater. Adv.*, 2025, **6**, 6109

Dye-integrated photocrosslinkable polymers and networks for the visual chromogenic detection of a bacterial enzyme†

Muhammad Atif,[a] Gizem Babuççu,[b] Martijn Riool,[bc] Sebastian A. J. Zaat[b] and Ulrich Jonas *[a]

Received 2nd June 2025,
Accepted 24th July 2025

DOI: 10.1039/d5ma00580a

rsc.li/materials-advances

In this work, a copolymer of poly[(hydroxy ethyl acrylamide)-*co*-(4-benzophenone acrylamide)-*co*-(hexamethylene diamine acrylamide)-*co*-(ECOSURF EH-3 acrylate)] was synthesized *via* free radical polymerization, followed by multi-step modification using click chemistry. The copolymer was subsequently functionalized with either 5-bromo-4-chloro-3-indolyl β-D-glucuronide (X-GLUC) or 4-nitrophenyl-β-D-glucuronide (PNPG), two enzyme-labile chromogenic substrates used to visually observe bacterial β-glucuronidase activity. This enzyme is secreted by over 98% of *Escherichia coli* strains, a common cause of healthcare-associated infections. The use of two substrates demonstrates the system's versatility in detecting β-glucuronidase activity across different bacterial species, wherein enzymatic cleavage of the dye-sugar bond produces a visible chromogenic signal. Both copolymers were found to be non-cytotoxic to human lung fibroblasts and were independently crosslinked under UV light to form distinct polymer network structures. Upon water swelling, each hydrogel enabled qualitative detection of β-glucuronidase-producing bacteria through the release of indigo or yellow dyes, corresponding to the chromogenic response of X-GLUC or PNPG, respectively. This colorimetric response was confirmed both visually and spectroscopically, underscoring the potential of these polymers for development into multiplexed enzyme-based bacterial detection platforms. The technology offers promising applications in microbiological diagnostics, particularly in food safety and medical contexts.

1 Introduction

Recent projections indicate that bacterial infections will cause 10 million deaths annually by 2050, surpassing the current mortality rate of cancer.[1] These infections can lead to inflammatory diseases such as pneumonia and meningitis.[2,3] Unfortunately, many of these infections are diagnosed only after becoming systemic or causing significant organ damage, complicating treatment and increasing costs due to high bacterial burdens.[4] Early detection tools for bacterial infections are urgently needed to reduce these risks.

In cases of potentially infected wounds, detection typically relies on clinical signs (*e.g.*, fever) and laboratory markers such as serum C-reactive protein levels and white blood cell counts.[5,6] For suspected wound infections, clinical microbiology laboratories conduct blood and wound swab analyses to identify pathogens. The diagnostic protocol usually involves bacterial cultivation followed by identification using MALDI-TOF mass spectrometry.[7,8] Advanced molecular techniques, such as real-time polymerase chain reaction (PCR),[9] are employed when specific non-culturable or slow growing pathogens are suspected. When initial results are inconclusive, sequencing of the 16S rDNA gene or even the entire genome is used for bacterial identification. However, these conventional methods have major limitations: they require culture for 24–48 hours or complex molecular diagnostic procedures, and wound sampling often necessitates dressing removal. The latter is contraindicated in cases such as second-degree burns where advanced dressings must remain undisturbed to allow skin regeneration.

Recent advances in bacterial detection technologies have introduced sophisticated laboratory methods, including optical endomicroscopy,[10] and confocal laser scanning microscopy with white light laser technology.[11] While these techniques provide reliable and rapid bacterial detection, their complexity, high costs, and requirement for specialized facilities limit their

[a] *Macromolecular Chemistry, Department of Chemistry and Biology, University of Siegen, Adolf-Reichwein-Strasse 2, 57076 Siegen, Germany. E-mail: jonas@chemie.uni-siegen.de*
[b] *Department of Medical Microbiology and Infection Prevention, Amsterdam UMC, Amsterdam institute for Immunology and Infectious Diseases, University of Amsterdam, Meibergdreef 9, 1105 AZ Amsterdam, The Netherlands*
[c] *Laboratory of Experimental Trauma Surgery, Department of Trauma Surgery, University Hospital Regensburg, Am Biopark 9, 93053 Regensburg, Germany*

† Electronic supplementary information (ESI) available. See DOI: https://doi.org/10.1039/d5ma00580a

utility outside hospital settings, driving research into alternative approaches.[12]

Nanomaterial-based approaches have shown promise for bacterial infection sensing. These include platforms such as nanoparticles,[7,8,10] nanocapsules (liposomes and polymersomes),[11,13–15] and nanopores or nanofibers.[16–20] Other innovative strategies utilize bacteria-targeting antibodies coupled to porous silicon,[17] microrobots,[21] microfluidics, microarrays,[22–24] nucleic acid-based molecular machines,[25–27] and polymer- or paper-based sensors.[28–30] Notable applications include flexible bandages with integrated temperature and pH sensors for *Staphylococcus aureus* detection,[31,32] which surpass traditional chromogenic culture methods.[33] Similarly, nanofibers and micro-bio-electronic devices have been developed for detecting *Escherichia coli*,[18,34] offering alternatives to standard methods.[35,36] This is of particular relevance, as *E. coli* is one of the most prevalent bacterial species found in healthcare-associated infections.[37]

Recent efforts have focused on developing rapid detection methods to overcome two key limitations: (i) time-consuming isolation steps and (ii) lengthy analyses. Given the wide range of clinically relevant bacterial species across medical, food production, and water safety applications, versatile and sensitive detection platforms are highly desired.[12] To address this, we present a novel approach for rapid *in situ* detection of bacterial enzymes. Our enzyme-sensing approach involves two modified hydrogels utilizing a biodegradable and biocompatible poly(*N*-hydroxyethylacrylamide)-based (PHEAAm) copolymer, which has demonstrated utility in various applications, including antifouling coatings, wound dressings, and drug delivery.[38] By expanding this strategy to other types of chromogenic substrates the technology may become potentially applicable to diagnostic wound dressings, biomedical devices, and food safety monitoring.

To develop this bacterial enzyme detection system (illustrated in Fig. 1), we focused on the enzyme β-glucuronidase (β-GUS) in *E. coli*. This enzyme catalyses the hydrolysis of β-linked D-glucopyranosiduronic acids to glucopyranosiduronic acid and aglycone.[39] β-GUS is present in approximately 98% of all known *E. coli* strains.[25] Although other bacterial species, including *Yersinia*, *Salmonella*, and *Shigella* species, can also produce β-GUS,[40,41] these organisms are rarely encountered in the context of wound infections treated with dressings.[42] Importantly, β-GUS production is regulated by bacterial density,[43] making it an effective indicator of colonization. In humans, the β-GUS enzyme is generally expressed intracellularly and thus unlikely to interfere with the proposed detection system for the bacterial enzyme.

In our design, we covalently immobilized the two chromogenic compounds 5-bromo-4-chloro-3-indolyl β-D-glucuronide (X-GLUC) and 4-nitrophenyl-β-D-glucuronide (PNPG) separately within the copolymer matrix. These substrates undergo specific enzymatic cleavage, releasing chromophores (an indole derivative and *p*-nitrophenol), resulting in visible colour changes detectable by the naked eye. This two-substrate approach enhances the accuracy and sensitivity of bacterial β-glucuronidase detection. As reported in the literature,[44–46] bacterial strains may differentially convert β-glucuronidase substrates, which is explained by structural variability in the peptide sequence of the β-glucuronidases, which underscores the value of using complementary systems. X-GLUC has previously been employed in polymer-based biosensing systems for β-glucuronidase detection, using traditional EDC/NHS chemistry with preformed polymer networks such as chitosan hydrogels[47] and sugar-based polyurethane foams.[48] In contrast, our photocrosslinking approach enables covalent integration of chromogenic dyes during polymer synthesis prior to network formation. The soluble polymers allow

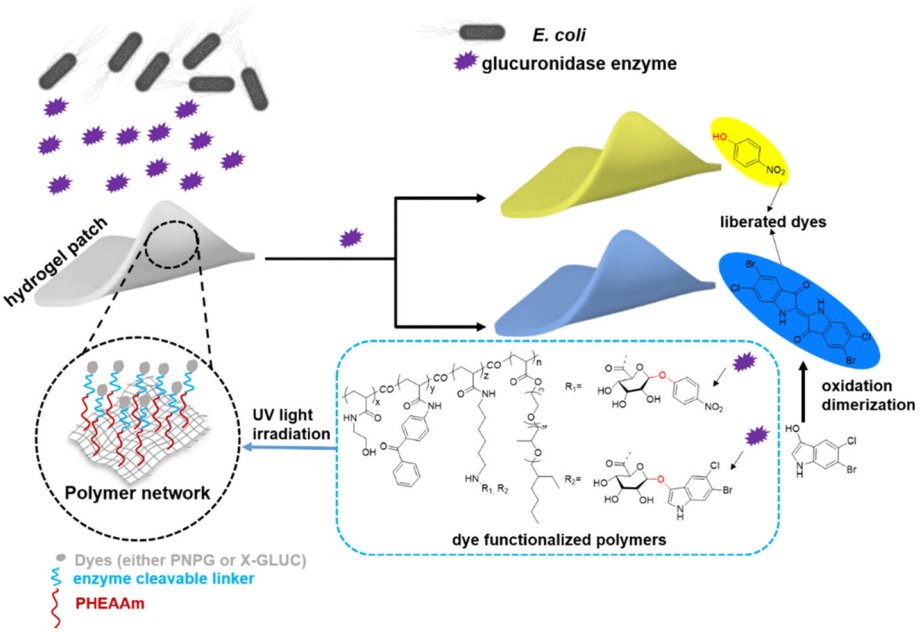

Fig. 1 Concept of colorimetric detection of bacteria based on the chromogenic response of dye-functionalized hydrogels.

full characterization of the chemical structure. Subsequent photocrosslinking provides improved spatial control over crosslinking density and a more uniform distribution of chromogenic dyes within the polymer network. Moreover, our dual-chromogenic substrate strategy achieves better coverage of potential variants, thereby improving the robustness and reliability of enzymatic detection. Such enzymatic reactions are valuable for microbiological applications, including monitoring metabolic processes and bacterial enzyme detection, which could ultimately lead to microbial screening applications.[49,50]

2 Experimental detail

2.1 Materials

All chemicals were obtained from commercial suppliers in Germany and used as received unless otherwise noted. *N*-(2-Hydroxyethyl)acrylamide (97%), pentafluorophenyl acrylate (PFPA; 98%), 4-nitrophenyl-β-D-glucuronic acid (PNPG; 99%), 5-bromo-4-chloro-3-indolyl β-D-glucuronic acid (X-GLUC; 99%) and laboratory-grade ECOSURF EH-3 (abbreviated as EH3) were purchased from Sigma-Aldrich. Azobisisobutyronitrile (AIBN) was recrystallized from methanol (98.5%; VWR Chemicals). Triethylamine (99.5%; Sigma-Aldrich) was distilled before use. 4-Benzophenone acrylamide (BPAAm) was synthesized according to the literature.[51] Hexamethylene diamine (97%; Sigma-Aldrich), and carbonyldiimidazole (97%; Alfa Aesar), were used as received. Trifluoroacetic acid (PEPTIPURE®; ≥99.9%) was purchased from Carl Roth. β-GUS isolated from *E. coli* (1000–5000 units per mg protein, E.C.3.2.1.31; type IX-A) was purchased from Sigma-Aldrich. Roswell Park Memorial Institute (RPMI) medium, supplemented with 20 mM Hepes and L-glutamine, without sodium bicarbonate (referred to as RPMI), was obtained from Sigma-Aldrich. Sodium dodecyl sulfate (SDS) was purchased from Sigma-Aldrich. Fetal bovine serum (FBS) and Dulbecco's modified Eagle medium (DMEM) were obtained from Thermo Fisher Scientific. Normal human lung fibroblasts (NHLF) were acquired from Lonza. Deionized water (Milli-Q) was used throughout the experiments.

2.2 Instruments

2.2.1 Nuclear magnetic resonance (NMR). ^{1}H NMR (500 MHz) and ^{19}F NMR (100 MHz) spectra were recorded on a Bruker AV 400 spectrometer at 25 ± 1 °C using deuterated chloroform ($CDCl_3$), deuterium oxide (D_2O), and deuterium dimethyl sulfoxide-d6 (DMSO-d6) as solvents. Tetramethylsilane (TMS) was used as an internal standard. 1D spectra were analysed with MestreNova 9 software.

2.2.2 Fourier-transform infrared spectroscopy (FTIR). FTIR spectra were recorded using a Bruker Tensor 27 spectrometer with a resolution of 2 cm^{-1} and a spectral range of 4000–400 cm^{-1}.

2.2.3 UV-Visible spectroscopy. UV-VIS spectra were recorded on a BioTek Epoch 2 IVD microplate spectrophotometer (Agilent) within the wavelength range of 300–700 nm and a scan rate of 300 nm min^{-1}, with automatic baseline correction applied.

2.3 Polymer synthesis

2.3.1 Synthesis of monomers. The acrylation of ECOSURF EH-3 yielded the surfactant monomer EH3A, following the protocol detailed in Scheme S1 (ESI†).[52] The ^{1}H NMR spectrum (Fig. S1, ESI†) confirmed the successful synthesis of EH3A. ^{1}H NMR (500 MHz, $CDCl_3$, T = 25 °C), δ ppm: 0.84 (t, 6H, 2x-CH_3), 1.12–1.25 (m, 20H, 4x-CH_3 and 4x-CH_2–), 1.47 (m, 1H, –CH–), 3.28–3.72 (m, 22H, 4x-CH–and 9x-CH_2–O–), 4.30 (m, 2H, –CH_2–O–), 5.81 (m, 1H, –CH═CH_2), 6.14 (m, 1H, –CH═CH_2), 6.41 (m, 1H, –CH═CH_2). The total integral of the area for the ^{1}H NMR peaks in the range of 5.8–6.5 ppm indicates a product purity of approximately 75%. The remaining 25% likely comprises unreacted starting materials (educts) and residual solvents. However, this impurity level is not expected to significantly affect the subsequent polymerization.

BPAAm, used as a photocrosslinker monomer, was synthesized as described in the literature,[51] and detailed in Scheme S2 (ESI†). The ^{1}H NMR spectrum (Fig. S2, ESI†) confirmed successful synthesis. ^{1}H NMR (500 MHz, $CDCl_3$, T = 25 °C), δ ppm: 5.70 (dd, 1H, H_2C═CHCONH–), 6.42 (dd, 1H, H_2C═CH–CONH–), 6.64 (dd, 1H, H_2C═CH–CONH–), 7.42 (m, 2H, -arom), 7.53 (m, 1H, -arom) and 7.74 (m, 6H, -arom). PFPA, an active ester monomer, was synthesized as reported previously[53] and detailed in Scheme S3 (ESI†). The ^{1}H NMR spectrum (Fig. S3, ESI†) confirmed successful synthesis. ^{1}H NMR (500 MHz, $CDCl_3$, T = 25 °C), δ ppm: 6.33 (dd, 1H, –CH═CH_2), 6.38 (dd, 1H, –CH═CH_2), 6.60 (dd, 1H, –CH═CH_2).

2.3.2 Synthesis of poly(HEAAm-*co*-BPAAm-*co*-PFPA-*co*-EH3A) and its modification with chromogenic dyes X-GLUC and PNPG. A copolymer was synthesized containing *N*-hydroxyethyl acrylamide (HEAAm) as a biocompatible main monomer, BPAAm as photocrosslinker monomer for hydrogel formation, EH3A as a surfactant for hydrophilic–hydrophobic balance and amphiphilicity, and PFPA as an active ester monomer for post-polymerization modification (PPM). The resultant copolymer, poly(HEAAm-*co*-BPAAm-*co*-PFPA-*co*-EH3A), was modified with hexamethylene diamine (HMDA) *via* active ester chemistry to form poly(HEAAm-*co*-BPAAm-*co*-HMDAAm-*co*-EH3A). This copolymer, containing free amines in its backbone, was subsequently modified with the chromogenic dyes X-GLUC and PNPG to produce poly(HEAAm-*co*-BPAAm-*co*-X-GLUC-*co*-EH3A) (PHXG) and poly(HEAAm-*co*-BPAAm-*co*-PNPG-*co*-EH3A) (PHPN), respectively.

2.3.2.1 Step 1 – synthesis of poly(HEAAm-co-BPAAm-co-PFPA-co-EH3A). In a Schlenk tube, 500 mg (4.41 mmol) of HEAAm, 72.60 mg (0.13 mmol) of EH3A, 22.20 mg (0.08 mmol) of BPAAm, 73.60 mg (0.30 mmol) of PFPA, and 7.25 mg (0.44 mmol, 1 mol%) of AIBN were combined (Fig. 2). Methanol (10 mL) was added, and the mixture was purged with argon before being heated at 65 °C for 24 h. The polymer was precipitated in diethyl ether, filtered, and dried under vacuum, yielding 67% of poly(HEAAm-*co*-BPAAm-*co*-PFPA-*co*-EH3A). Characterization by ^{1}H NMR, ^{19}F NMR, and FTIR (Fig. S6–S8, ESI†) confirmed successful synthesis. ^{1}H NMR (500 MHz, DMSO, T = 25 °C), δ ppm: 0.8–2.25 (EH3A and polymer backbone), 2.8–3.7 (ethyl group of HEAAm), 4.6–5.2 (–OH protons of

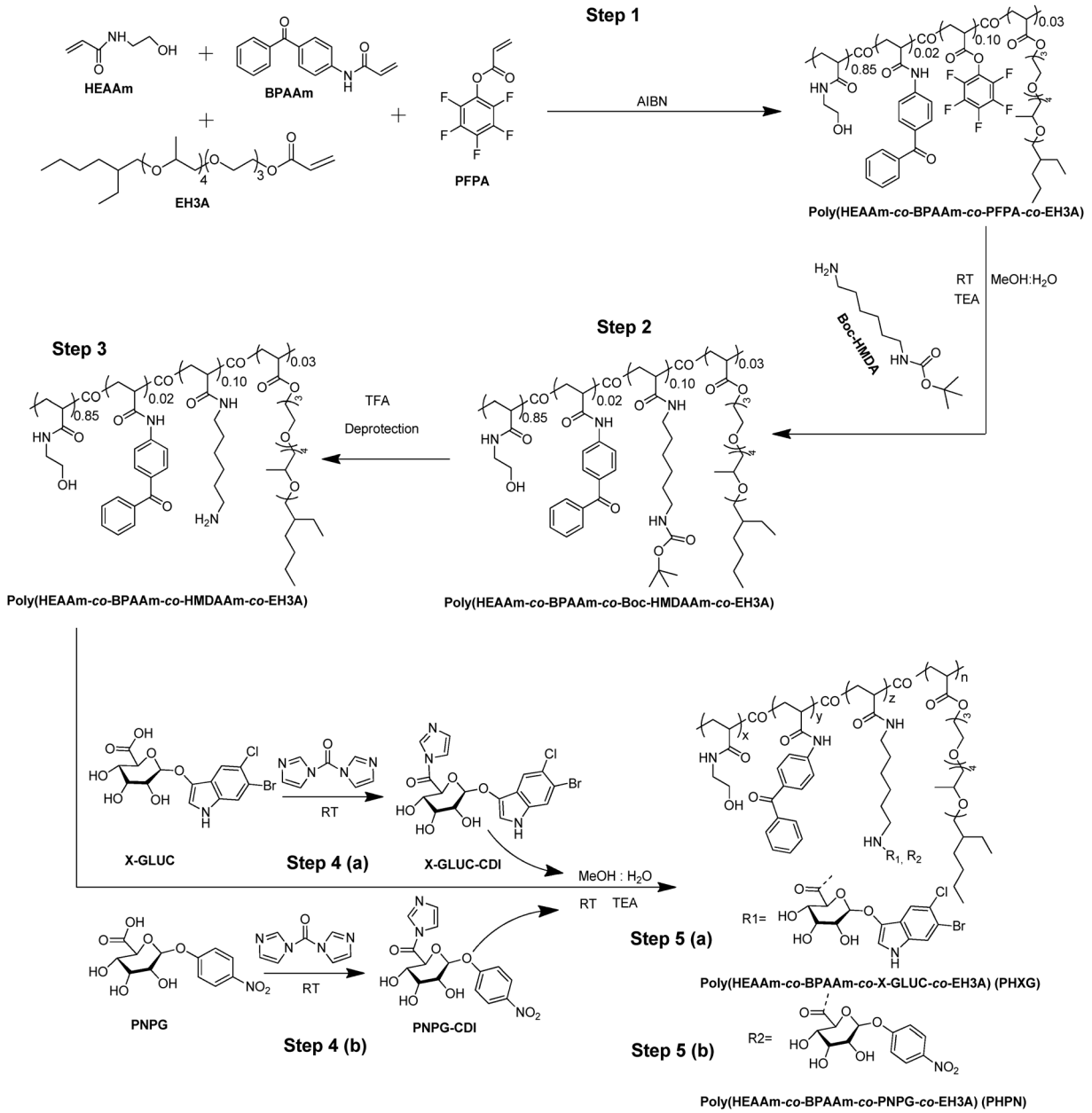

Fig. 2 Synthesis strategy of poly(HEAAm-*co*-BPAAm-*co*-X-GLUC-*co*-EH3A) (PHXG) and poly(HEAAm-*co*-BPAAm-*co*-PNPG-*co*-EH3A) (PHPN), respectively. Abbreviations used in this strategy are azobisisobutyronitrile (AIBN), triethyl amines (TEA), methanol (MeOH), trifluoro acetic acid (TFA), and room temperature (RT). This is referred to as ''strategy 1'' in Section 3.1 Polymer synthesis.

HEAAm), 7.2–8.0 (aromatic proton of BPAAm side group units and amide protons of HEAAm). ^{19}F NMR (500 MHz, DMSO), δ (ppm): −162/−164 (2F) (pentafluorophenyl, *meta*), −156/−158 (1F) (pentafluorophenyl, *para*), −150/−154 (2F) (pentafluorophenyl, *ortho*). FT-IR (cm^{-1}): 1100–1270 (C–F), 1600–1650 (aromatic ring), 1725–1750 (C═O).

2.3.2.2 Step 2 – conjugation with Boc-protected HMDA. In a Schlenk tube, 250 mg (1.05 mmol) of poly(HEAAm-*co*-BPAAm-*co*-PFPA-*co*-EH3A) (synthesized in step 1) was mixed with 159 mg (0.73 mmol, 10 eq.) of *N*-*tert*-butyloxycarbonyloxy (Boc)-protected HMDA (Boc-HMDA) and 7.4 μL of triethylamine (TEA) in 10 mL of a methanol : chloroform (8 : 1) solvent mixture. The mixture was stirred at room temperature for 120 h, then precipitated in acetone, filtered, dried, redissolved in water, dialyzed, and finally freeze-dried, yielding 64% of poly(HEAAm-*co*-BPAAm-*co*-Boc-HMDAAm-*co*-EH3A). Characterization by ^{1}H NMR and ^{19}F NMR confirmed successful synthesis (Fig. S9 and S10, ESI†). ^{1}H NMR (500 MHz, DMSO, T = 25 °C), δ ppm: 0.8–2.25 (EH3A and polymer backbone), 1.1–1.2 (Boc protected unit), 2.8–3.7 (ethyl group of HEAAm), 4.6–5.2 (–OH protons of HEAAm), 7.2–8.0 (aromatic proton of BPAAm side group units and amide protons of HEAAm). The absence of the PFPA ester peak in ^{19}F NMR indicated successful coupling of HDMA.

2.3.2.3 Step 3 – deprotection of Boc groups. The Boc-protected polymer (100 mg) was dissolved in 1.5 mL of methanol, and 1.5 mL of trifluoroacetic acid (TFA) was added to deprotect the amine groups. The reaction mixture was stirred overnight, then precipitated in ice-cold acetone, filtered, redissolved in water, and freeze-dried. The product was further purified using Lewatit MP62 for anion exchange, yielding poly(HEAAm-*co*-BPAAm-*co*-HMDAAm-*co*-EH3A). The disappearance of Boc peaks (1.1–1.2 ppm) in ^{1}H NMR confirmed successful deprotection (Fig. S9 and S11, ESI†).

2.3.2.4 Step 4 – activation of chromogenic dyes. (a) X-GLUC-CDI: 150 mg (0.33 mmol) of X-GLUC and 76 mg (0.47 mmol, 1.4 eq.) of carbonyldiimidazole (CDI) were dissolved in 10 mL of Milli-Q water and stirred at room temperature for 120 h. The reaction mixture was washed with 10 mL of dichloromethane, the aqueous phase was separated, and the product was freeze-dried, yielding 83% of X-GLUC-CDI. ^{1}H NMR confirmed successful synthesis (Fig. S12, ESI†). ^{1}H NMR (500 MHz, DMSO, T = 25 °C), δ ppm: 3.40–3.78 (sugar unit), 4.65–7.90 (imidazole and indole derivative protons). (b) PNPG-CDI: 47 mg (0.14 mmol) of PNPG and 36 mg (0.22 mmol) of CDI were dissolved in 10 mL of Milli-Q water and stirred at room temperature for 120 h. The reaction mixture was then washed with 10 mL of dichloromethane, the aqueous phase was separated, and the product was freeze-dried, yielding 72% of PNPG-CDI. ^{1}H NMR confirmed successful synthesis (Fig. S13, ESI†). ^{1}H NMR (500 MHz, DMSO, T = 25 °C), δ ppm: 3.50–3.90 (sugar unit), 5.25–8.35 (imidazole and nitrophenol protons).

2.3.2.5 Step 5 – polymer modification with dyes. (a) PHXG (X-GLUC-modified polymer): 50 mg (0.07 mmol) of poly(HEAAm-*co*-BPAAm-*co*-HMDAAm-*co*-EH3A) and 50.93 mg (0.11 mmol, 5 eq.) of X-GLUC-CDI were dissolved in 10 mL of Milli-Q water with 4 μL of TEA. The mixture was stirred at room temperature for 72 h, precipitated in ice-cold acetone, redissolved in water and freeze-dried, yielding 75% of poly(HEAAm-*co*-BPAAm-*co*-X-GLUC-*co*-EH3A), abbreviated as PHXG. ^{1}H NMR confirmed successful synthesis (Fig. 3a). ^{1}H NMR (500 MHz, DMSO, T = 25 °C), δ ppm: 0.8–2.25 (EH3A and polymer backbone), 2.8–3.7 (ethyl group of HEAAm), 4.5 (sugar unit), 4.6–5.2 (–OH protons of HEAAm), 7.0–7.9 and 10.75 (aromatic proton of BPAAm side group units and amide protons of HEAAm, and chromogenic substance X-GLUC). (b) PHPN (PNPG-modified polymer): 50 mg (0.07 mmol) of poly(HEAAm-*co*-BPAAm-*co*-HMDAAm-*co*-EH3A) and 55.10 mg (0.15 mmol, 5 eq.) of PNPG-CDI were dissolved in 10 mL of Milli-Q water with 3 μL of TEA. This mixture was stirred at room temperature for 72 h, precipitated in ice-cold acetone, redissolved in water, and freeze-dried, yielding 59% of poly(HEAAm-*co*-BPAAm-*co*-PNPG-*co*-EH3A), abbreviated as PHPN. ^{1}H NMR confirmed successful synthesis (Fig. 3b). ^{1}H NMR (500 MHz, DMSO, T = 25 °C), δ ppm: 0.8–2.25 (EH3A and polymer backbone), 2.8–3.7 (ethyl group of HEAAm), 4.6–5.2 (–OH protons of HEAAm), 5.4 (sugar unit), 7.0–8.3 (aromatic proton of BPAAm side group units and amide protons of HEAAm, and chromogenic substance PNPG).

2.4 Hydrogel formation

To prepare hydrogel films, dye-modified polymers were dissolved in a methanol–water mixture (90 : 10, v/v) at a concentration of 25 mg mL^{-1}. The solution was poured into a Petri dish and dried on a hotplate at 40 °C overnight. The resulting polymer films were exposed to UV light at a wavelength of 365 nm (1 h = 13.0 J cm^{-2}) for 30 min to induce crosslinking and form a surface-attached polymer network. Subsequent swelling in water produced the final hydrogel. A similar process was followed to create hydrogel films in 96-well plates. These immobilized hydrogel films were used for UV-VIS absorption analysis and microbiological experiments.

2.5 Bacterial culture

Prior to the experiments, clinical and laboratory strains of *E. coli* (PC 1568, PC 2348AR4, DH5α, B12C1, DC10B,[54] TOP10,[55] ATCC 8739,[56] and ML35 (ATCC 43827)),[57] *S. aureus* strain JAR060131,[58] a standard laboratory strain of *Pseudomonas aeruginosa* PAO1, and a multidrug-resistant strain of *Acinetobacter baumannii* RUH875[59] were grown from frozen stocks at 37 °C on blood agar plates (BioMerieux) for 16–18 h. Subsequently, overnight cultures were prepared in lysogeny broth (LB; Oxoid) for all *E. coli* strains and in tryptic soy broth (TSB; Oxoid) for *S. aureus*, *P. aeruginosa*, and *A. baumannii*. These cultures were incubated at 37 °C for 18–24 h with shaking at 120 rpm. Prior to each experiment, bacteria were cultured to the mid-logarithmic phase in their respective media for 3 h at 37 °C with shaking at 120 rpm. Cultures were washed twice with phosphate-buffered saline (PBS; 140 mM NaCl, pH 7; Sigma-Aldrich) and diluted in Roswell Park Memorial Institute 1640 medium (RPMI) to a final concentration of 1 × 10^6 colony forming units (CFU) per mL, based on optical density measurements at 620 nm.

2.6 Chromogenic effect of enzyme solution on dye-modified polymers in solution and on surface-attached hydrogels

2.6.1 Visual observations. To evaluate the enzymatic effect on the soluble polymers, 1 mL of dye-modified separate polymer solutions (PHXG or PHPN) were prepared in PBS (pH 7) at a concentration of 25 mg mL^{-1} and added to separate glass vials. Freshly prepared β-GUS solution (10 μL) in PBS was added to each PHXG and PHPN polymer solution vial, at a final enzyme concentration of 0.1 μM (3 replicates each). Visual colour changes were monitored.

The chromogenic effect was also examined on hydrogels made from PHXG and PHPN. Fresh enzyme solution (10 μL of β-GUS at 0.1 μM concentration in PBS, pH 7) was prepared and added to PHXG and PHPN hydrogels. Colour changes were observed visually (3 replicates each).

2.6.2 UV-VIS spectral study. For this experiment, 100 μL of dye-modified polymer solutions (PHXG and PHPN; 25 mg mL^{-1} in PBS, pH 7) were added to a 96-well plate. The solutions were dried using a microwave oven and immobilized by photocrosslinking. The resulting polymer network was washed with PBS (pH 7) solution to remove any non-crosslinked polymers or

impurities, then dried under vacuum for 1 h at 40 °C. Fresh enzyme solution (10 μL of β-GUS at 0.1 μM concentration in PBS, pH 7) was added separately to the wells containing PHXG and PHPN hydrogels. The 96-well plate was immediately inserted into a UV-VIS spectrophotometer microplate reader for analysis[60,61] (3 replicates each).

2.7 Assessment of colorimetric bacterial detection using dye-modified single chain polymers in solutions

For this study, 100 μL of dye-modified polymer solutions (PHXG and PHPN) were added to each well of 96-well plates, followed by the addition of 100 μL of bacterial suspension (1×10^6 CFU per mL). The plates were incubated overnight at 37 °C (2 replicates each). After incubation, colour changes were observed visually and analysed using UV-VIS spectroscopy.

2.8 WST-1 assay

For this experiment, 0.1–5 × 10^4 NHLF cells per well were cultured in a 96-well microtiter plate with a final volume of 100 μL DMEM supplemented with 2% FBS. The cells were incubated for 24 h, after which the medium was replaced with 100 μL fresh DMEM with 2% FBS. Two-fold serial dilutions of pure polymer (without dye modification) and dye-modified polymer solutions (25 mg mL^{-1}; 2 replicates each; final volume of 100 μL) were added to separate wells and incubated for an additional 24 h. Subsequently, 10 μL of WST-1 reagent (Roche) was added to each well and incubated for 30 min. Afterwards, the media changed colour from pink to yellowish. The reaction was stopped by adding 10 μL of 1% SDS to each well, followed by shaking the plate for 1 min to mix the contents. Absorbance of the untreated control and treated samples was measured using a microplate reader (Synergy H1, Biotek, USA) at 400 nm. A blank control containing 100 μL culture medium with 10 μL WST-1 was included in separate wells.

3 Results and discussion

This study aimed to develop a polymer-based sensor for rapid bacterial detection based on a chromogenic response. The sensor utilizes dye-modified polymers that release distinctly coloured products upon enzymatic cleavage of labile bonds by a bacterial enzyme. These colour changes, observable with the naked eye either in polymer solution or in a hydrogel, provide a reliable and easy-to-interpret signal for bacterial presence.

3.1 Polymer synthesis

A copolymer of poly[(hydroxyethyl acrylamide)-*co*-(4-benzophenone acrylamide)-*co*-(pentafluorophenyl acrylate)-*co*-(ECOSURF EH-3 acrylate)] was synthesized *via* free radical polymerization, as shown in step 1 of Fig. 2. Post-polymerization modification (PPM) with hexamethylene diamine (HMDA) introduced primary amine functionality into the polymer backbone (steps 2 and 3; Fig. 2). These free amines served as functional sites for subsequent modification with dye derivatives (steps 4 and 5; Fig. 2). The final dye-modified polymers were crosslinked under UV light and swollen in water to form hydrogels. Both solution-phase and hydrogel forms of the polymers released distinct coloured products upon enzymatic cleavage, indicating the presence of bacteria.

The acrylate-based monomers for copolymer synthesis were prepared according to established protocols. The copolymer poly(HEAAm-*co*-BPAAm-*co*-PFPA-*co*-EH3A) consisted of four distinct monomers. Pentafluorophenyl acrylate (PFPA) served as an activated ester for PPM with primary amines.[53] ECOSURF EH-3 acrylate (EH3A), a surfactant monomer, provided amphiphilic properties.[52] 4-Benzophenone acrylamide (BPAAm) acted as a photocrosslinking monomer, enabling the formation of crosslinked polymer networks upon UV exposure.[51] *N*-Hydroxyethyl acrylamide (HEAAm) was the primary hydrophilic and biocompatible monomer.[62]

The synthesized copolymer was characterized using ^{1}H NMR (Fig. S6, ESI†), ^{19}F NMR (Fig. S7, ESI†), and FTIR (Fig S8, ESI†). The ^{1}H NMR spectrum confirmed successful synthesis of the copolymer, with no unreacted monomer remaining. The spectrum exhibited signals corresponding to the polymer backbone and EH3A in the chemical shift δ range of 0.8–2.25 ppm, the ethyl group of HEAAm at 2.8–3.7 ppm, the –OH protons of HEAAm at 4.6–5.2 ppm, the aromatic protons of the BPAAm side groups and amide protons of HEAAm at 7.2–8.0 ppm. The solvent (from d6-DMSO) peak appears around 2.5 ppm, as shown in Fig. S6 (ESI†). Furthermore, the three distinct chemical shifts observed in the ^{19}F NMR spectra in the range of −162/−164 ppm (*meta*), −156/−158 ppm (*para*), and −150/−154 ppm (*ortho*) are indicative of a pentafluorophenyl ring, verifying the presence of the active ester (PFPA) unit within the copolymer, as represented in Fig. S7 (ESI†). Additionally, the FTIR spectrum exhibits a strong band in the range of 1100–1270 cm^{-1}, indicative of C–F stretching vibrations, further supporting the presence of a fluorinated moiety. A band observed between 1600 and 1650 cm^{-1} is consistent with aromatic ring stretching, while the band at 1725–1750 cm^{-1} suggests the presence of a carbonyl group (C═O), as shown in Fig. S8 (ESI†).

Active esters in the polymer backbone were functionalized with Boc-protected hexamethylene diamine (Boc-HMDA) in step 2, yielding poly(HEAAm-*co*-BPAAm-*co*-Boc-HMDAAm-*co*-EH3A). ^{1}H NMR (Fig. S9, ESI†) confirmed the presence of a new peak at 1.1–1.3 ppm, indicating successful incorporation of Boc-protected units. Deprotection of the Boc groups in step 3 yielded poly(HEAAm-*co*-BPAAm-*co*-HMDAAm-*co*-EH3A), with the absence of the 1.1–1.3 ppm peak (Fig. S11, ESI†) confirming successful deprotection.

In step 4, chromogenic dyes (X-GLUC and PNPG) were activated with CDI to form their respective active esters. ^{1}H NMR of X-GLUC-CDI (Fig. S12, ESI†) revealed peaks at 3.40–3.65 ppm and 4.60 ppm (sugar unit) and 6.60–7.85 ppm (imidazole and aromatic groups). Similarly, PNPG-CDI (Fig. S13, ESI†) displayed peaks at 3.50–3.65 ppm and 5.20–5.29 ppm (sugar unit) and 7.00–8.25 (imidazole and nitrophenol groups). These dyes were coupled with the copolymer in step 5 to form PHXG and PHPN, as confirmed by ^{1}H NMR spectra (Fig. 3a and b). In the spectrum of PHXG in Fig. 3a, the polymer backbone and EH3A signals are visible in the range of

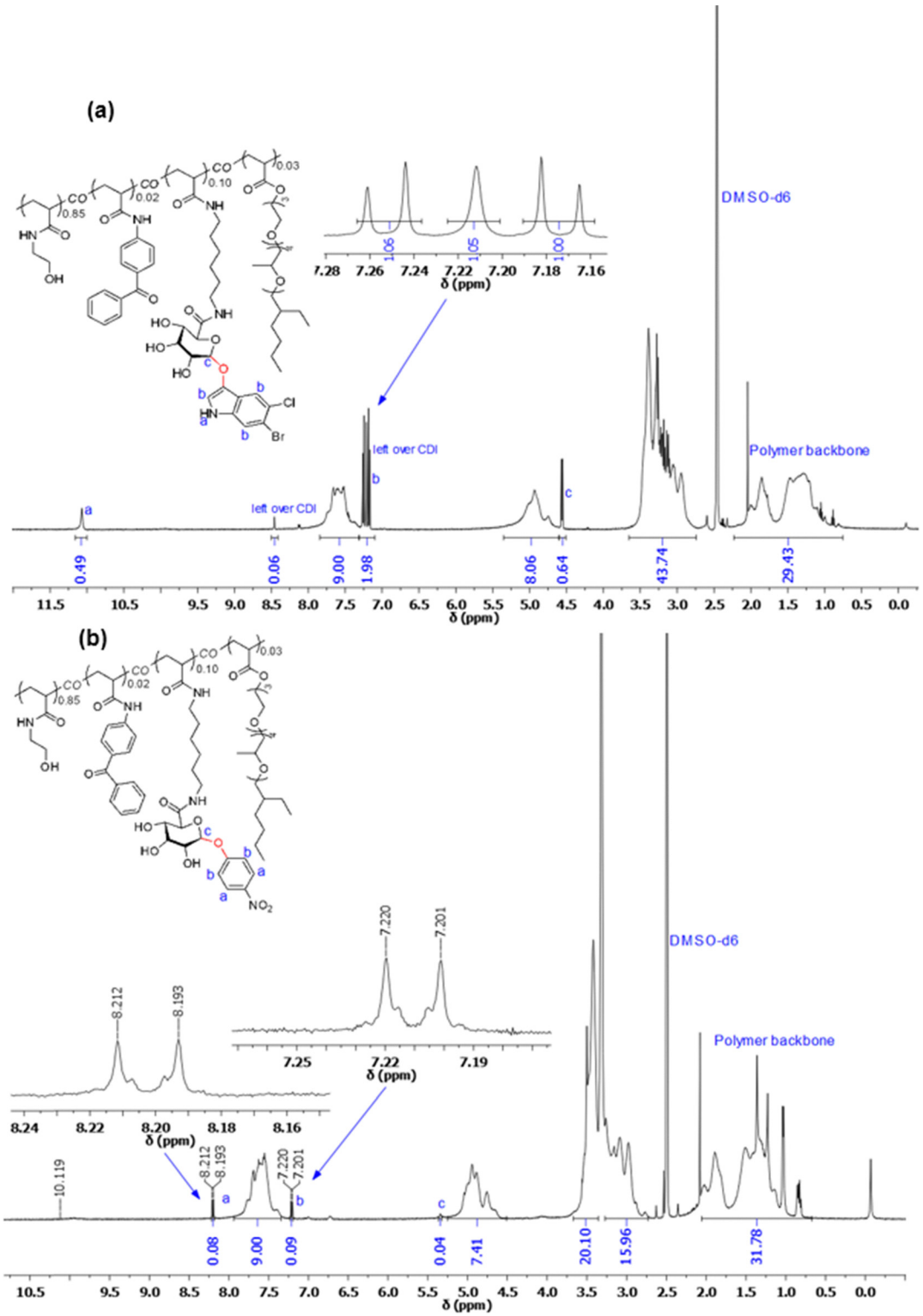

Fig. 3 ^{1}H NMR spectra (measured at room temperature in $CDCl_3$, Larmor frequency: 500 MHz) of (a) poly(HEAAm-*co*-BPAAm-*co*-X-GLUC-*co*-EH3A) (b) poly(HEAAm-*co*-BPAAm-*co*-PNPG-*co*-EH3A).

0.7–2.1 ppm. The ethyl group of HEAAm is located between 2.7 and 3.8 ppm, while the –OH protons of HEAAm appear between 4.3 and 5.4 ppm. Aromatic protons from the BPAAm side groups and amide protons of HEAAm are observed at 7.4–7.9 ppm. The solvent DMSO contributes a peak around 2.5 ppm. The sugar unit of X-GLUC appears at 4.5–5.0 ppm, and the chromogenic fragment 5-bromo-4-chloro-3-indolyl β-D-glucuronide gives rise to peaks between 7.1 and 8.3 ppm,

with an additional peak at 10.75 ppm. Similarly, the ^{1}H NMR spectrum of PHPN in Fig. 3b displays peaks attributed to the polymer backbone and EH3A (0.7–2.1 ppm), the HEAAm ethyl group (2.7–3.8 ppm), its –OH protons (4.3–5.4 ppm), and the combined aromatic protons of BPAAm side groups and HEAAm amide protons (7.4–7.9 ppm). The DMSO solvent peak occurs around 2.5 ppm. Additionally, the bands of the sugar unit from PNPG lie at 5.3–5.4 ppm, while the chromogenic fragment 4-nitrophenyl shows peaks between 7.0 and 8.3 ppm. Alternative synthetic strategies were evaluated (Fig. S4 and S5, ESI†). Strategy 2 involved initial coupling of PNPG and X-GLUC derivatives with Boc-HMDA, followed by deprotection and subsequent modification with the copolymer. However, steric hindrance reduced coupling efficiency, and purification proved challenging in this strategy. Strategy 3 employed the copolymerization of acrylate-based monomers, including Boc-HMDAAm, followed by deprotection and subsequent coupling with CDI-activated dyes. Although this strategy simplified some steps, yields were lower compared to strategy 1, particularly during precipitation in step 1. Therefore, strategy 1 was chosen for further experiments for its higher yield and simpler purification.

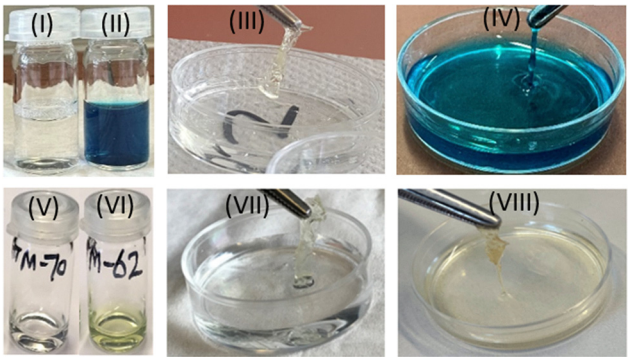

Fig. 4 Visual tests of enzymatic activity for the chromogenic polymer systems PHXG and PHPN. No colour changes were observed for the reference polymer PHEAAm after adding the enzyme β-GUS (I) and (V) in Milli-Q water. In contrast, the polymer solutions of PHXG and PHPN, containing the chromogenic substances X-GLUC (II) and PNPG (VI), exhibited distinct colour changes upon enzyme addition. Similarly, no colour change occurred in the reference hydrogels of PHEAAm (III and VII), whereas the hydrogels from PHXG and PHPN, containing X-GLUC (IV) and PNPG (VIII), showed characteristic colour changes following enzyme addition. Triplicate samples were tested (n = 3) and representative samples are shown.

3.2 Chromogenic effect of enzyme on dye-modified polymer solutions and on surface-attached hydrogels

β-GUS is secreted by more than 98% of known *E. coli* strains.[12,63] Although some strains of *Yersinia*, *Salmonella*, *Shigella*, *Aerococcus viridans*, *Bacillus* spp., or *Corynebacterium* are also capable of producing β-GUS,[40,41] these bacteria are rarely encountered in wound dressing applications.[42] In this study, commercially available β-GUS (1000–5000 units per mg protein, E.C.3.2.1.31; type IX-A) isolated from *E. coli*, was used to evaluate the chromogenic effect on dye-modified polymers in solutions and surface-attached hydrogels. In the polymer containing X-GLUC (PHXG), the β-linked indole derivative of X-GLUC is cleaved by β-GUS and dimerizes to form 5,5′-dibromo-6,6′-dichloro-indigo, an insoluble compound with a distinctive indigo colour. The chromogenic response can be visually detected, as shown in Fig. 4(II). In the polymer containing PNPG (PHPN), β-GUS cleaves the glucuronide, liberating 4-nitrophenol (4-NP). The corresponding yellow colour, caused by deprotonation of 4-NP, becomes evident after the enzymatic reaction, as depicted in Fig. 4(VI). A comparative analysis was conducted between dye-modified polymers in solution (PHXG and PHPN), and a reference polymer, poly(HEAAm-*co*-BPAAm-*co*-EH3A) (PHEAAm), which lacks chromogenic substances and served as control. As illustrated in Fig. 4(I) and (V), the control solution (PHEAAm) exhibited no colour change upon enzyme addition. In contrast, PHXG and PHPN solutions developed indigo and yellow colours, respectively, demonstrating that the chromogenic substances remain active when covalently immobilized within the polymer backbone and cleaved during enzymatic reaction with β-GUS. The chromogenic effect was also tested in hydrogels prepared from photocrosslinked PHXG and PHPN. Similar to the solutions, the chromogenic substances within the hydrogels were cleaved by the enzymes, resulting in the formation of indigo and yellow colours, respectively. This confirms that the chromogenic substances retain their activity after immobilization within the polymer network and remain accessible to the enzyme *via* diffusion through the hydrogel matrix. The results are presented in Fig. 4(IV) and (VIII), alongside the hydrogel derived from PHEAAm, which again served as a control (Fig. 4(III) and (VII)).

3.3 UV-VIS spectral study of the chromogenic effect of enzyme on dye-modified hydrogels

The chromogenic effect of the enzyme solution of β-GUS on dye-modified hydrogels with X-GLUC and PNPG incorporated was analysed using UV-VIS spectroscopy (Fig. S14, ESI†). The spectrum of the hydrogel containing X-GLUC (PHXG) in Fig. S14(a) (ESI†) shows increased absorption in the wavelength range of 550–700 nm. This increase corresponds to the formation of the dimerized indigo derivative, a result of β-GUS enzymatically cleaving the chromogenic indole species from the hydrogel. To track reaction over time, absorption spectra were recorded during 20 consecutive cycles of enzymatic reaction with a 20-minute interval between each cycle. The time-*versus*-absorbance plot at 620 nm (inset, Fig. S14(b), ESI†) demonstrates a continuous increase in absorption over the reaction period ($>$300 min). These findings confirm that the enzyme diffuses into the swollen hydrogel matrix and cleaves the glycosidic bond near the polymer backbone. During this process, the hydrogel immobilized in the well plates turned indigo (Fig. S14(c), ESI†).

A similar response was observed with the hydrogel PHPN containing PNPG (Fig. S14(d), ESI†). An absorption peak at 400 nm emerged, indicating the formation of 4-NP as a result of the enzymatic reaction between the PNPG and β-GUS diffusing into the hydrogel matrix. Absorption spectra were collected over 20 consecutive enzymatic reaction cycles, with 20-minute intervals between cycles. Absorption at 400 nm steadily increased, reflecting the ongoing formation of 4-NP (Fig. S14(e), ESI†). This process also resulted in a visual colour change, with the

hydrogels turning yellow (Fig. S14(f), ESI†). Furthermore, Fig. S14(c) and (f) (ESI†) show that no colour change was observed in the PHXG and PHPN polymers dissolved in PBS without the addition of pure enzyme, clearly indicating that the chemically immobilized chromogenic dyes in the polymer backbone remain stable in the PBS buffer solution. This lack of colour development confirms that the β-linked D-glucopyranosiduronic acid moieties were not hydrolyzed under these conditions and that both X-Gluc and PNPG remained chemically stable within the crosslinked hydrogel networks. To further assess potential dye leaching, the hydrogels were thoroughly washed with PBS (pH 7.4) to remove any unreacted monomers, residual impurities, and non-covalently bound dyes. The emergence of a chromogenic response only after enzymatic exposure confirms that the dyes remained covalently immobilized within the polymer matrix and with no detectable leaching during the incubation period.

3.4 Chromogenic response of dye-modified single chain polymer solutions to bacteria

In the following experiment, the chromogenic effect of the two dye-modified polymers in solution was tested with live bacteria. Due to known variations in the structure of β-GUS from different bacterial species and strains of single species that result in different activities and substrate specificities,[44–46] we designed two separate chromogenic polymers, PHXG and PHPN. These two polymer substrates are expected to show individual enzyme susceptibilities by different variants of β-GUS and thus cover a broader range of bacterial species and strains. *E. coli* strains DC10B, B12C1, TOP10, PC.

2348AR4, ATCC 8739, and ML35 induced a distinct indigo colour when incubated with PHXG as shown in Table 1. This indicates the sufficient production of β-GUS by these strains to cleave the chromogenic dye. In contrast, no colour change was observed in PHPN solutions exposed to these bacterial strains, indicating a higher sensitivity of the X-GLUC- than of the PNPG-modified polymers in solution to detect enzymatic activity. Interestingly, *E. coli* strain PC 1568 only induced a yellow colour change in PHPN solutions, but no colour change of the PHXG solution indicating β-GUS activity with higher affinity towards PNPG. Additionally, strain DH5α triggered chromogenic responses in both PHXG and PHPN solutions, indicating the production of β-GUS enzyme with sufficient affinity towards both X-GLUC and PNPG.

No colour change was observed in PHXG or PHPN solutions when exposed to either *S. aureus* (JAR060131), *P. aeruginosa* (PAO1), or *A. baumannii* (RUH875), suggesting either the lack of enzyme production (which is expected for these species), expression of β-GUS variants that have no affinity for the chromogenic polymers, or insufficient secretion of β-GUS for detectable chromogenic changes in this assay. Our findings demonstrate that the polymer-based chromogenic systems PHXG and PHPN are effective for detecting a wide range of *E. coli* strains, with characteristic colorimetric responses based on the enzymatic activity. This also confirms the advantage of using two different chromogenic polymers, which provides better coverage of detection of β-GUS activity across diverse *E. coli* strains, aligning with the reports that more than 98% of *E. coli* produce this enzyme.[12,63]

Table 1 Enzymatic reaction study of various strains of *E. coli*, *S. aureus*, *P. aeruginosa*, and *A. baumannii*, in aqueous solutions of the dye-modified polymers PHXG and PHPN. PBS was taken as negative control and PHEAAm polymer was taken as reference polymer. Duplicate samples were tested, one representative sample is shown, with both yielded highly similar results

Strain	Enzymatic activity of β-GUS	
	PHXG	PHPN
E. coli DC10B	+	-
E. coli B12C1	+	-
E. coli TOP10	+	-
E. coli PC2348AR4	+	-
E. coli ATCC8739	+	-
E. coli ML35	+	-
E. coli PC1568	-	+
E. coli DH5α	+	+
S. aureus JAR060131	-	-
A. baumannii RUH875	-	-
P. aeruginosa PAO1	-	-

Indigo and yellow colour with (+) sign signal the production of β-glucuronidase (β-GUS) enzyme as detected by PHXG and PHPN, respectively. No color with (−) sign shows the absence of β-GUS enzyme.

3.5 UV-VIS spectral study of the chromogenic efficacy of bacteria by dye-modified polymers in solution

Following the visual detection of bacterial enzyme activity through the chromogenic effect on PHXG and PHPN polymer solutions, the chromogenic activity was further evaluated using UV-VIS spectroscopy, as shown in Fig. 5 and Fig. S15 (ESI†). The absorbance spectra of PHXG solutions incubated with *E. coli* strains DC10B, B12C1, TOP10, PC 2348AR4, ATCC 8739, and ML35 showed strong absorption peaks within the range of 550–680 nm, confirming their production of β-GUS enzyme. These findings align with the indigo colour change observed visually (Fig. 4) and in UV-VIS analysis (Fig. S14(c), ESI†) when PHXG had been treated with pure β-GUS enzyme solution. Similarly, a peak at 400 nm in the spectrum of PHPN solution with *E. coli* PC 1568 confirmed the secretion of β-GUS, consistent with the yellow colour change observed visually in bacterial suspensions with PHPN solution (Fig. 5 and Fig. S14, ESI†). Notably, the UV-VIS spectrum of *E. coli* strain DH5α exhibited both peaks (400 nm and 550–680 nm), indicating the production of β-GUS and its affinity towards both X-GLUC and PNPG. This observation matches the colour changes seen in both PHXG and PHPN solutions treated with DH5α (Table 1). In contrast, the UV-VIS spectra of *S. aureus* JAR060131, *P. aeruginosa* PAO1, and *A. baumannii* RUH875 showed no significant peaks (Fig. 5). The absence of peaks suggests that these strains do not produce detectable levels of β-GUS enzyme, consistent with the absence of visible colour changes (Table 1), as generally expected for these bacterial species.

3.6 Cytotoxicity

The viability of human lung fibroblasts exposed to solutions of dye-modified polymers PHXG and PHPN, as well as the reference polymer PHEAAm (without dye modification), was evaluated using the WST-1 assay. This assay relies on the conversion of the tetrazolium salt WST-1 to formazan by mitochondrial dehydrogenases. The conversion rate is directly proportional to the number of viable cells, as active mitochondria produce more dehydrogenase enzymes. The amount of formazan produced is quantified by measuring absorbance at 400 nm. As shown in Fig. 6, over 70% of cells maintained metabolic activity after exposure to dye-modified polymer solutions up to a concentration of 25 mg mL^{-1}. These results indicate low toxicity, meeting the requirements of the international standard ISO 10993-5:2009 for medical devices.[64]

Overall, the study demonstrates that the developed dye-modified copolymers, both in solution and hydrogel form, can effectively detect β-GUS, through visible chromogenic responses. These findings suggest that the copolymers could be used to manufacture detection systems that enable on-site detection of bacterial contamination. Moreover, unlike more complex techniques such as MALDI-TOF mass spectrometry or PCR, our system does not require specialized equipment nor extensive training. Owing to their simple and visible readout, the hydrogels made from these copolymers could also be integrated into wound dressings for continuous monitoring of bacterial infections. By using a two-chromogenic substrate approach with eight different *E. coli* strains, we achieved better

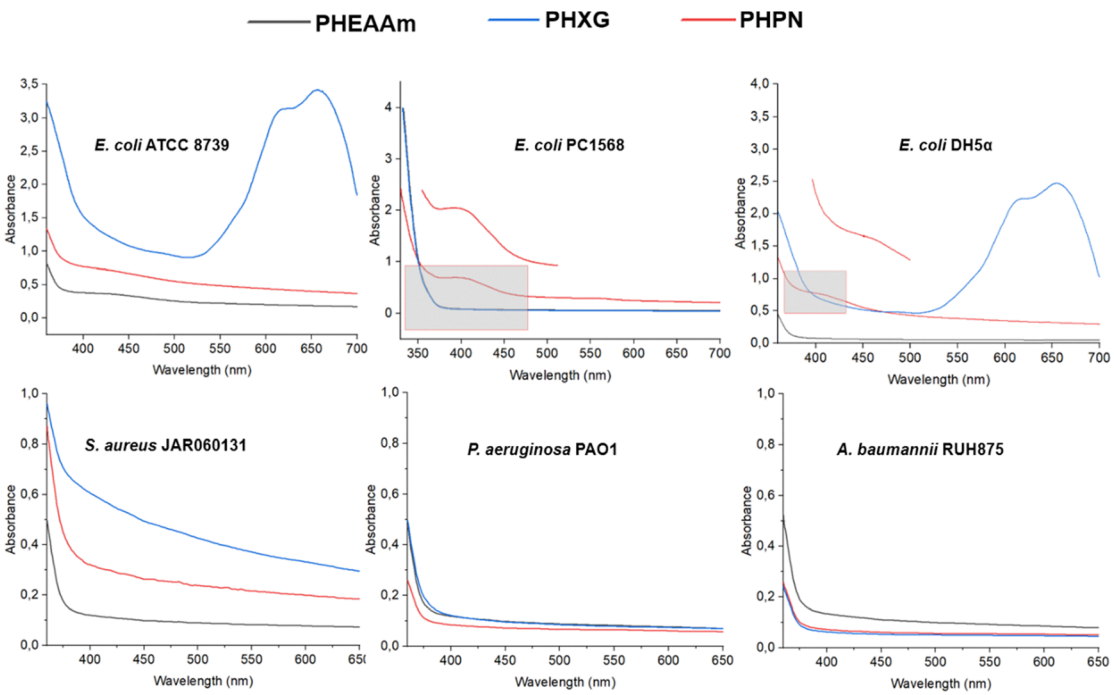

Fig. 5 UV-VIS absorption spectra of dye-modified polymer solutions for the PHEAAm reference and the chromogenic systems PHXG and PHPN, after incubation with different strains of *E. coli*, *S. aureus*, *P. aeruginosa*, and *A. baumannii*. Duplicate samples were tested, and one representative sample is shown, with both yielding similar results.

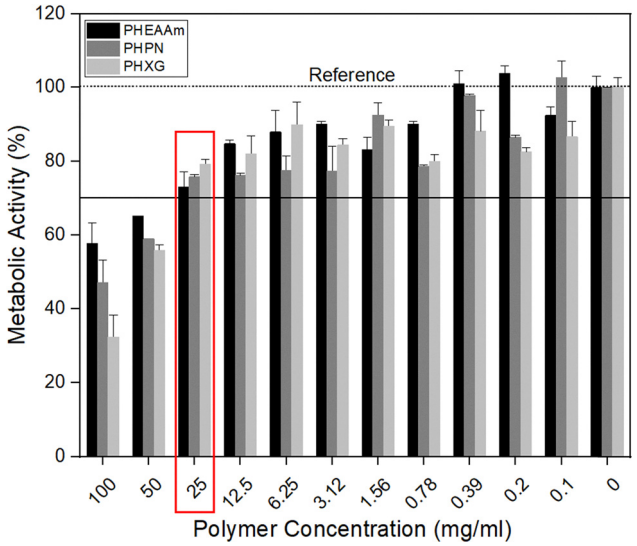

Fig. 6 Analysis of metabolic activity using the WST-1 assay for NHLF cells in contact with solutions of single-chain polymers without dye modification (PHEAAm) and with dye modification (PHXG and PHPN). The solid black line indicates the 70% cut-off value for viability. Values represent mean percentage metabolic activity + SD. Duplicate samples were tested.

coverage of potential β-GUS variants, thereby improving the robustness and reliability of enzymatic detection. However, our system detects only β-GUS, so a lack of colour change could mean a false negative result in case non-β-GUS producing *E. coli* strains would be present. This limitation should be considered, and further research is needed to explore the potential for multiplexing with other dye substrates that are sensitive to different enzymes of *E. coli* to further increase coverage of different strains. Separately, while the present study focused on demonstrating the feasibility of visible chromogenic detection, future work should also include quantitative evaluation of this chromogenic-modified hydrogels. In particular, determining the limit of detection (LOD) and assessing sensitivity under biologically and clinically relevant conditions will be essential for advancing the system toward practical applications. An estimation for LOD in our system could be based on the results provided in the literature where *E. coli* suspensions with concentrations of 5.8×10^7 CFU per mL were detected within 6.2 h using enzyme-responsive hydrogel-coated paper documented *via* a smartphone camera.[47] Moreover, extension of the substrates to detect other enzymes may be a strategy to broaden the range of detectable pathogens not only in wound infection but also in biomedical devices and food safety monitoring.

4 Conclusion

In this study, we successfully developed and characterized photocrosslinkable copolymers, poly(HEAAm-*co*-BPAAm-*co*-X-GLUC-EH3A) and poly(HEAAm-*co*-BPAAm-*co*-PNPG-*co*-EH3A), which demonstrated no cytotoxicity to human lung fibroblasts up to the concentration of 25 mg mL^{-1}. These copolymers, and the hydrogels derived from them, provide a convenient method for direct visual observation of β-GUS enzyme activity in enzyme solutions as well as in bacterial suspensions. The covalently immobilized chromogenic substances X-GLUC and PNPG retained their capacity to be converted by the enzyme within the UV-crosslinked polymer network, enabling chromogenic reactions without interference. The enzymatic cleavage of these chromogenic dyes produced distinct indigo and yellow colour changes, respectively, which is observable with the naked eye. Our two polymer-based sensor system effectively detected the bacterial glucuronidase enzyme, either as purified protein or from growing bacterial cells, showcasing its potential as a promising detection platform. The results further highlight the benefit of employing a two-polymer-based approach, which enhance qualitative detection reliability and broadens the coverage of β-GUS activity among diverse *E. coli* strains. However, to enable future medical applications across various sample matrices, further validation of appropriate immobilization methods and assessment of the detection approach will be required for different, wound environments. Similarly, for food contamination analysis and water quality monitoring the performance of our detection systems will need to be investigated under relevant biological and practical settings.

Conflicts of interest

Yes. Patent application has been submitted on 31.10.2024 to the EPO with application number EP 24 210 082.4.

Data availability

The data supporting this article have been included as part of the ESI.†

Acknowledgements

We greatly acknowledge the financial support from the European Union's Horizon 2020 research and innovation programme under the Marie SKŁODOWSKA-CURIE grant STIMULUS (agreement No. 955664). We thank Dr. Emelie Alsheim, Dr. Naing Tun Thet, and Prof. Dr. A. Toby A. Jenkins from the Department of Chemistry, University of Bath, Bath, UK, for their valuable discussions and assistance during initial microbiological training, as well as Dr. Thomas Paululat and Ali Balasini from the Department of Chemistry and Biology, University of Siegen, Siegen, Germany, for the NMR measurements and extensive discussions.

References

1 A. L. Furst and M. B. Francis, *Chem. Rev.*, 2018, **119**, 700–726.
2 C.-H. Song, *JBV*, 2013, **43**, 85–91.
3 D. M. Monack, A. Mueller and S. Falkow, *Nat. Rev. Microbiol.*, 2004, **2**, 747–765.
4 A. Zlitni, G. Gowrishankar, I. Steinberg, T. Haywood and S. Sam Gambhir, *Nat. Commun.*, 2020, **11**, 1250.

5 J. C. Rodríguez-Sanjuán, J. I. Martín-Parra, I. Seco, L. García-Castrillo and A. Naranjo, *Dis. Colon Rectum*, 1999, **42**, 1325–1329.
6 M. Khan, E. Davie and K. Irshad, *J. Ayub Med. Coll. Abbottabad*, 2004, **16**, 1–6.
7 C. Y. Zhang, J. Gao and Z. Wang, *Adv. Mater.*, 2018, **30**, 1803618.
8 H. Peng and I. A. Chen, *ACS Nano*, 2018, **13**, 1244–1252.
9 H. D. VanGuilder, K. E. Vrana and W. M. Freeman, *Biotechniques*, 2008, **44**, 619–626.
10 T. Mocan, C. T. Matea, T. Pop, O. Mosteanu, A. D. Buzoianu, C. Puia, C. Iancu and L. Mocan, *J. Nanobiotechnol.*, 2017, **15**, 1–14.
11 R. Sum, M. Swaminathan, S. K. Rastogi, O. Piloto and I. Cheong, *ACS Sens.*, 2017, **2**, 1441–1451.
12 M.-M. Sadat Ebrahimi, Y. Voss and H. Schönherr, *ACS Appl. Mater. Interfaces*, 2015, **7**, 20190–20199.
13 S. Milo, N. T. Thet, D. Liu, J. Nzakizwanayo, B. V. Jones and A. T. A. Jenkins, *Biosens. Bioelectron.*, 2016, **81**, 166–172.
14 S. Haas, N. Hain, M. Raoufi, S. Handschuh-Wang, T. Wang, X. Jiang and H. Schönherr, *Biomacromolecules*, 2015, **16**, 832–841.
15 Y. Li, X. Hu, D. Ding, Y. Zou, Y. Xu, X. Wang, Y. Zhang, L. Chen, Z. Chen and W. Tan, *Nat. Commun.*, 2017, **8**, 15653.
16 C.-K. Joung, H.-N. Kim, M.-C. Lim, T.-J. Jeon, H.-Y. Kim and Y.-R. Kim, *Biosens. Bioelectron.*, 2013, **44**, 210–215.
17 Y. Tang, Z. Li, Q. Luo, J. Liu and J. Wu, *Biosens. Bioelectron.*, 2016, **79**, 715–720.
18 P. M. Shaibani, H. Etayash, K. Jiang, A. Sohrabi, M. Hassanpourfard, S. Naicker, M. Sadrzadeh and T. Thundat, *ACS Sens.*, 2018, **3**, 815–822.
19 J. P. Yapor, A. Alharby, C. Gentry-Weeks, M. M. Reynolds, A. M. Alam and Y. V. Li, *ACS Omega*, 2017, **2**, 7334–7342.
20 H. Zhang, J. Lv and Z. Jia, *Sensors*, 2018, **18**, 105.
21 Y. Zhang, L. Zhang, L. Yang, C. I. Vong, K. F. Chan, W. K. Wu, T. N. Kwong, N. W. Lo, M. Ip and S. H. Wong, *Sci. Adv.*, 2019, **5**, eaau9650.
22 V. Templier, T. Livache, S. Boisset, M. Maurin, S. Slimani, R. Mathey and Y. Roupioz, *Sci. Rep.*, 2017, **7**, 9457.
23 W. Lee, D. Kwon, W. Choi, G. Y. Jung, A. K. Au, A. Folch and S. Jeon, *Sci. Rep.*, 2015, **5**, 1–7.
24 Z. Altintas, M. Akgun, G. Kokturk and Y. Uludag, *Biosens. Bioelectron.*, 2018, **100**, 541–548.
25 M. Xiao, K. Zou, L. Li, L. Wang, Y. Tian, C. Fan and H. Pei, *Angew. Chem., Int. Ed.*, 2019, **58**, 15448–15454.
26 H. Yu, M. Xiao, W. Lai, M. F. Alam, W. Zhang, H. Pei, Y. Wan and L. Li, *Anal. Chem.*, 2020, **92**, 4491–4497.
27 H. Yang, M. Xiao, W. Lai, Y. Wan, L. Li and H. Pei, *Anal. Chem.*, 2020, **92**, 4990–4995.
28 M. M. Ali, C. L. Brown, S. Jahanshahi-Anbuhi, B. Kannan, Y. Li, C. D. Filipe and J. D. Brennan, *Sci. Rep.*, 2017, **7**, 12335.
29 Z. A. I. Mazrad, I. In, K.-D. Lee and S. Y. Park, *Biosens. Bioelectron.*, 2017, **89**, 1026–1033.
30 Z. Li, R. Paul, T. Ba Tis, A. C. Saville, J. C. Hansel, T. Yu, J. B. Ristaino and Q. Wei, *Nat. Plants*, 2019, **5**, 856–866.
31 M. Laabei, W. D. Jamieson, R. C. Massey and A. T. A. Jenkins, *PLoS One*, 2014, **9**, e87270.
32 P. Mostafalu, A. Tamayol, R. Rahimi, M. Ochoa, A. Khalilpour, G. Kiaee, I. K. Yazdi, S. Bagherifard, M. R. Dokmeci and B. Ziaie, *Small*, 2018, **14**, 1703509.
33 V. Compernolle, G. Verschraegen and G. Claeys, *J. Clin. Microbiol.*, 2007, **45**, 154–158.
34 M. Mimee, P. Nadeau, A. Hayward, S. Carim, S. Flanagan, L. Jerger, J. Collins, S. McDonnell, R. Swartwout and R. J. Citorik, *Science*, 2018, **360**, 915–918.
35 L. Durso and J. Keen, *J. Appl. Microbiol.*, 2007, **103**, 2457–2464.
36 J. J. Hirvonen, A. Siitonen and S.-S. Kaukoranta, *J. Clin. Microbiol.*, 2012, **50**, 3586–3590.
37 S. Szabó, B. Feier, D. Capatina, M. Tertis, C. Cristea and A. Popa, *J. Clin. Med.*, 2022, **11**, 3204.
38 C. Zhao, K. Patel, L. M. Aichinger, Z. Liu, R. Hu, H. Chen, X. Li, L. Li, G. Zhang and Y. Chang, *RSC Adv.*, 2013, **3**, 19991–20000.
39 S. Aich, L. T. Delbaere and R. Chen, *Biotechniques*, 2001, **30**, 846–850.
40 F. Molina, E. López-Acedo, R. Tabla, I. Roa, A. Gómez and J. E. Rebollo, *BMC Biotechnol.*, 2015, **15**, 1–9.
41 L. Fiksdal, M. Pommepuy, M.-P. Caprais and I. Midttun, *Appl. Environ. Microbiol.*, 1994, **60**, 1581–1584.
42 W. D. Watkins, S. R. Rippey, C. R. Clavet, D. J. Kelley-Reitz and W. Burkhardt 3rd, *Appl. Environ. Microbiol.*, 1988, **54**, 1874–1875.
43 J. W. Leung and Y. Liu, *Gastroenterology*, 2003, **4**, A247.
44 S. C. Edberg and C. M. Kontnick, *J. Clin. Microbiol.*, 1986, **24**, 368–371.
45 S. J. Pellock, B. C. Creekmore, W. G. Walton, N. Mehta, K. A. Biernat, A. P. Cesmat, Y. Ariyarathna, Z. D. Dunn, B. Li and J. Jin, *ACS Cent. Sci.*, 2018, **4**, 868–879.
46 A. LoGuidice, B. D. Wallace, L. Bendel, M. R. Redinbo and U. A. Boelsterli, *J. Pharmacol. Exp. Ther.*, 2012, **341**, 447–454.
47 K. Kaur, W. Chelangat, S. I. Druzhinin, N. W. Karuri, M. Müller and H. Schönherr, *Biosensors*, 2021, **11**, 25.
48 M. Santos, I. Tiago, M. Mariz, P. Ferreira and S. Alarico, *Mater. Today Chem.*, 2024, **40**, 102193.
49 M. Manafi, W. Kneifel and S. Bascomb, *Microbiol. Rev.*, 1991, **55**, 335–348.
50 S. Orenga, A. L. James, M. Manafi, J. D. Perry and D. H. Pincus, *J. Microbiol. Methods*, 2009, **79**, 139–155.
51 B. Peng, Z. Tong, W. Y. Tong, P. J. Pasic, A. Oddo, Y. Dai, M. Luo, J. Frescene, N. G. Welch and C. D. Easton, *ACS Appl. Mater. Interfaces*, 2020, **12**, 56753–56766.
52 S. Freese, S. Diraoui, A. Mateescu, P. Frank, C. Theodorakopoulos and U. Jonas, *Gels*, 2019, **6**, 1.
53 P. Theato, *J. Polym. Sci., Part A: Polym. Chem.*, 2008, **46**, 6677–6687.
54 P. Redder and P. Linder, *Appl. Environ. Microbiol.*, 2012, **78**, 3846–3854.
55 M. T. Worthington, R. Q. Luo and J. Pelo, *Biotechniques*, 2001, **30**, 738–742.
56 P. Broxton, P. Woodcock and P. Gilbert, *J. Appl. Microbiol.*, 1983, **54**, 345–353.

57 R. Lehrer, A. Barton, K. A. Daher, S. Harwig, T. Ganz and M. E. Selsted, *J. Clin. Invest.*, 1989, **84**, 553–561.
58 D. Campoccia, L. Montanaro, T. Moriarty, R. Richards, S. Ravaioli and C. R. Arciola, *Int. J. Artif. Organs*, 2008, **31**, 841–847.
59 L. Dijkshoorn, H. Aucken, P. Gerner-Smidt, P. Janssen, M. Kaufmann, J. Garaizar, J. Ursing and T. Pitt, *J. Clin. Microbiol.*, 1996, **34**, 1519–1525.
60 H.-U. Bergmeyer, *Methods of enzymatic analysis*, Elsevier, 2012.
61 T. Tephly, M. Green, B. Coffman, C. King, Z. Cheng and G. Rios, *Advances in pharmacology*, Elsevier, 1997, vol. 42, pp. 343–346.
62 M. Ashaduzzaman, S. C. Dey, M. K. Hossain and A. Tiwari, *Polym. Bull.*, 2024, 1–17.
63 D. Kim, Y. Jin, E. Jung, M. Han and K. Kobashi, *Biol. Pharm. Bull.*, 1995, **18**, 1184–1188.
64 S. Atefyekta, E. Blomstrand, A. K. Rajasekharan, S. Svensson, M. Trobos, J. Hong, T. J. Webster, P. Thomsen and M. Andersson, *ACS Biomater. Sci. Eng.*, 2021, **7**, 1693–1702.